Computer Assisted Mechanics and Engineering Sciences, 14: 91–106, 2007.

Simulation of traffic flow through a toll gate

Hikaru Shimizu[1], Akemi Hara[2], Tatsuhiro Tamaki[3], Eisuke Kita[1]

[1] *Graduate School of Information Science, Nagoya University*

[2] *School of Informatics and Sciences, Nagoya University*

[3] *Ube National College of Technology*

(Received June 15, 2005)

This paper describes the simulation of the traffic flow through toll gate. A two-lane road is considered as the object domain and then, the local rules are defined to control the vehicle behavior. First, one simulates the traffic flows through the road with two non-ETC gates or the road with two ETC gates. The maximum traffic amount on the roads with two ETC gates is less than that on the road without gates by about 10%, while, in the case of the roads with two non-ETC gates, the maximum traffic amount decreases by 80%. Next, one simulates the traffic flows through the road with one non-ETC gate and one ETC gate. The traffic amount depends not only on the vehicle occupancy but also on the percentage of ETC vehicles among all driving vehicles.

Keywords: traffic flow, toll gate, traffic cognition, stochastic velocity model, cellular automata

1. Introduction

Recently, the massive increase of the traffic amount in the urban city causes several social problems such as the traffic congestion, environmental pollution and so on. For overcoming the problems, the simulation system for the traffic flow attracts the attention widely as the key issue at the next stage of the intelligent transportation system (ITS). The traffic flow simulation is very important not only for the settlement of the traffic congestion but also from the viewpoint of the city design and the environmental engineering [10, 20, 30].

The traffic congestion is caused by several occasions; e.g., the entrance of the tunnel, the sag point where the road gradient changes, the toll gate and so on. The toll gate is one of the most popular reasons for the traffic congestion and the statistical data tell us that 30% of the total traffic congestion rise at the toll gates. Therefore, the Electronic Toll Collection System (ETC) has been developed with a vigorous effort.

In this paper, the traffic flow simulator based on the cellular automata and the stochastic velocity model [25] is applied to the simulation of the traffic congestion at the toll gate. The stochastic velocity model (SVM), which has been developed in our research group, performs the movement and the velocity change of the vehicle according to the random number. Since, in the SVM, the maximum movement of the vehicle is up to one cell at each time step, the rules to control the vehicle behavior are simpler than the previous studies. The authors have successfully applied the SVM to the traffic flow simulation on the freeway and the urban city [25, 26]. In this study, the model is applied to the simulation of the traffic flow at the toll gates.

The paper is organized as follows. In Section 2, the simulation models for the traffic flow are compared and the stochastic velocity model is also introduced. In Section 3, the simulation algorithm is explained by defining the object domain, the local rules to control vehicles. The numerical examples are shown in Section 4 and the results are concluded in Section 5.

2. Background

2.1. Macro- and micro-models

The traffic flow simulation models are classified mainly into macro- and micro-models [24, 32].

In the macro-model, the traffic flow is though to be the liquid flow and its behavior is modeled with the constitutive equation. Lighthill and Whitham have presented one-dimensional model for the traffic flow in 1950s [15]. Musha *et al.* have also presented the model based on the Bergers equation [16]. In the micro-model, the behavior of each vehicle is controlled individually by the computer and then, the mutual interference between the vehicles constitutes the traffic flow [24].

Since, in the macro-model simulation, the traffic flow is represented with the constitutive equation, the computational cost is much cheaper than the micro-model simulation.

However, the comparison of the macro-model simulation results with the real traffic data has revealed that the traffic flow strongly depends on the individual characteristics of individual vehicles [27]. Therefore, some researchers have been studying the traffic simulation based on the micro-model such as the fuzzy theory, the cellular automata, the multi-agent model and so on. This is because the micro model simulation can represent the individual characteristics of the vehicles.

2.2. Micro-model simulation

In the micro-model, the behavior of each vehicle is controlled individually by the computer and then, the mutual interference between the vehicles constitutes the traffic flow [13, 24]. The key-point of the micro-model is how to represent the velocity change of the vehicle. In the previous studies, the velocity change of the vehicles is represented by the number of the cells which the vehicle moves at each time step.

2.2.1. Rule-184 CA model

The first traffic simulation model, which was based on the rule-184 named by Wolfram [32], simulated vehicles moving on one-lane freeway. The vehicles move at constant velocity and do not accelerate even when the distance between vehicles is very far. The rule-184 CA model cannot simulate the actual traffic flows well.

2.2.2. Nagel–Schreckenberg model

The Nagel Schreckenberg (NaSch) model is composed of the rule-184 CA model and the rules for acceleration and deceleration of vehicles [5, 7, 12, 14, 17–19, 21, 22, 28, 29].

In the model, the vehicle velocity is represented by the number of cells v which a vehicle moves at each time step. Assuming that the feasible maximum velocity and the present velocity of a vehicle are referred respectively as $v_{\max}$ and v ($v < v_{\max}$), the vehicle velocity v is changed according to the distance from a forehand vehicle *GAP*.

The vehicle velocity in the NaSch model is represented with the number of cells v that the vehicle moves at a time step. When the model is applied to the freeway traffic flow simulations, the fact that vehicles move over multi-cells at a time step results in the reduction of computational cost. When, however, it is applied to urban city traffic flow, the behavior rules of the vehicles become very complicated due to the existence of the traffic signals, the intersections and the branch lines.

Recently, NaSch model has been applied to the other simulation than the traffic flow such as the pedestrian, the social system and so on [2, 6, 11].

2.2.3. Vehicle (car) following model

In the vehicle following model, the vehicle velocity is determined from the distance or the velocity difference between a vehicle and the forehand one. The velocity v or the acceleration a of the vehicle are calculated from the following equations [1, 3, 24, 31, 33].

$$v \propto \Delta x,$$
$$a \propto \frac{v^m}{[\Delta x]^l} \Delta v,$$
$$a \propto V[\Delta x] - v,$$

where Δx and Δv denote the distance and the velocity difference between the vehicle and the forehead vehicle, respectively. m and l are parameters specified in advance. Besides, $V[\Delta x]$ is the optimal velocity function [24]. The simulation model using the optimal velocity function is called as the optimal velocity model.

In the vehicle following models, the velocity or the acceleration is represented as a continuous functions of the distance and the velocity difference between the vehicle and the forehead vehicle. Therefore, the velocity change in the vehicle following model is much more minute than the NaSch model. Note that, however, there exits the same difficulty as the NaSch model in the case of the traffic flow simulations in urban cities.

2.2.4. Biham–Middleton–Levine model

Biham *et al.* have presented the cellular automata model for simulating the traffic flow in urban cities [4, 9]. The roads in an urban city are expressed as a tetragonal lattice and vehicles can move only in upward or rightward directions. Three different traffic control models are presented in the BML model. In the BML-I, vehicles move in vertical direction at odd time step and in horizontal direction at even time step, respectively. That demonstrates the traffic flow in a urban city controlled by traffic signals. In the BML-II, all vehicles move simultaneously in both directions and when vehicles meet at the intersections, the vehicles going into intersections are selected at random. In the BML-III, all vehicles move simultaneously in both directions, like as BML-II model, and when the vehicles meet at the intersections, both vehicles can go into intersections simultaneously.

The BML model is the first idea for the traffic flow simulations in urban cities. Note that, however, it is too simple for actual traffic flow simulations in urban cities.

2.2.5. Stochastic velocity model

The vehicle behavior rules in the above micro models are generally very complicated because a vehicle velocity is represented by the number of cells that the vehicle passes over for a time-step. If there exists an obstacles such as a stopped vehicle and the traffic signal on the passed cells, the velocity and the behavior of the vehicle should be controlled in order to stop before the obstacles.

For overcoming the difficulty, the authors have presented the "Stochastic Velocity Model (SVM)". In the SVM, the vehicle movement is controlled with uniform random number and the number of the cell which the vehicle moves for one time step is up to one cell. Therefore, the rules for the vehicle movement are simpler than the existing studies. The SVM has been successfully applied to the traffic flow simulation on the highway and the urban city [25, 26].

In the SVM, the vehicle movement is controlled as follows. The velocity and the maximum velocity of the vehicle i are referred to as v^i and $v^i_{\max}$ ($v^i < v^i_{\max}$). The movement of the vehicle is represented as follows:

1. The parameter P^i is calculated as

$$P^i = \frac{v^i}{v^i_{\max}} . \tag{1}$$

2. The uniform random number $P(x)$ generates from 0 to 1.
3. If $P(x) < P^i$, the vehicle moves by one cell.
4. The process is repeated at each time step.

3. Simulation algorithm

The simulation model is based on the cellular automata. In the cellular automata simulation, the object domain is divided into small square cells and then, the state at each cell is updated according to the local rules from the state of the updated cell and its neighborhood cells.

In this section, we will define the cell representation of the object domain, the state variables at the cells and the local rules. The local rules are mainly classified into the behavior, the velocity, and the movement local rules. The behavior local rule controls the vehicle behavior such as the lane changing. The velocity local rules are classified into the absolute and the relative velocity local rules. The absolute velocity local rule decelerates the vehicle velocity to the toll gate, while the relative velocity local rule changes the vehicle velocity according to the distance between the vehicles.

3.1. Object domain

The two-lane road is considered as the object domain (Fig. 1). Each lane is defined by aligning 300 cells in a line. Since the size of a cell is 3 m × 3 m, the lane length is 900 m. The length of the toll gate is four cells (12 m).

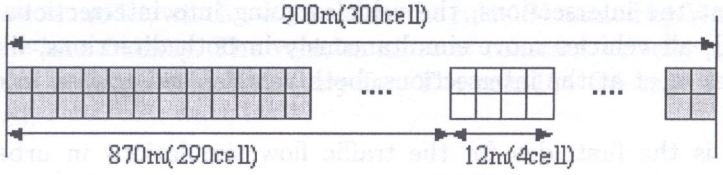

Fig. 1. Object domain

3.2. State variables for road cell

The state variable at each cell is defined by the vehicle number and three road variables such as the road type, the road direction and the road occupancy. The road state variables are shown in Table 1.

The variable S_1 means the road type. The road of $S_1 = 1, 2, 3, 5, 6, 7$ and 8 denote thru traffic lane, left turn lane, right turn lane, the non-ETC toll gate, ETC toll gate, red signal, road shoulder and obstacles, respectively.

The variable S_2 means the road direction. The road of $S_2 = 1, 2, 3$ and 4 denote the road on which the vehicles move in the northern, the western, the eastern and the southern directions, respectively. The road of $S_2 = 7$ and 8 denote that the cells are occupied with a red signal and the other ones than a road, a driving vehicle and a signal, respectively.

Table 1. State variables on road cell

S_1	S_2	S_3	Description
1	1	0	Thru traffic lane in northern direction
1	2	0	Thru traffic lane in western direction
1	3	0	Thru traffic lane in eastern direction
1	4	0	Thru traffic lane in southern direction
2	1	0	Left turn lane in northern direction
2	2	0	Left turn lane in western direction
2	3	0	Left turn lane in eastern direction
2	4	0	Left turn lane in southern direction
3	1	0	Right turn lane in northern direction
3	2	0	Right turn lane in western direction
3	3	0	Right turn lane in eastern direction
3	4	0	Right turn lane in southern direction
8	8	8	No road and obstacles
7	7	7	Red signal
5	*	*	non-ETC toll gate
6	*	*	ETC toll gate

Finally, the variable S_3 means the road occupancy. If the cell is occupied with a vehicle, $S_3 = 1$. If not so, $S_3 = 0$. In case of $S_3 = 7$, a red signal is on the cell. In case of $S_3 = 8$, the cell is occupied with the other ones than a road, a driving vehicle and a red signal such as an obstacle.

3.3. State variables for vehicle

The state variables specified for the vehicle consist of the velocity v^i, the maximum velocity $v^i_{\max}$, the acceleration rate $\alpha^1 i$ and the vehicle following distance G. By the way, the vehicle following distance means the distance between the target vehicle and its forehand vehicle.

3.4. Safety following vehicle distance

In the study, it is assumed that the vehicle is driven so as to maintain the vehicle following distance G^i in the safety vehicle following distance G^i_s. The safety vehicle following distance G^i_s is determined as the function depending the velocity v from the actual data as follows [26],

$$G^i_s = 0.0029v^2 + 0.3049v\,. \tag{2}$$

As shown in [26], the vehicle following distance and the velocity have been estimated from the actual vehicles driving on the Nagoya–Nagakute avenue in City of Nagoya, Japan. The driving vehicles were recorded into the video tape and the velocity and the vehicle following distance were esteemed from the video. Equation (2) was determined from the least square approximation of the data.

The parameters G^i_0, G^i_r, and G^i_l mean the vehicle following distance on the lane on which the vehicle i drives and its right-hand and the left-hand neighbor lanes, respectively (Fig. 2).

3.5. Local rule

The local rules consist of the behavior, the velocity and the movement local rules. The local rules are applied to all vehicles in the order as shown in Fig. 3.

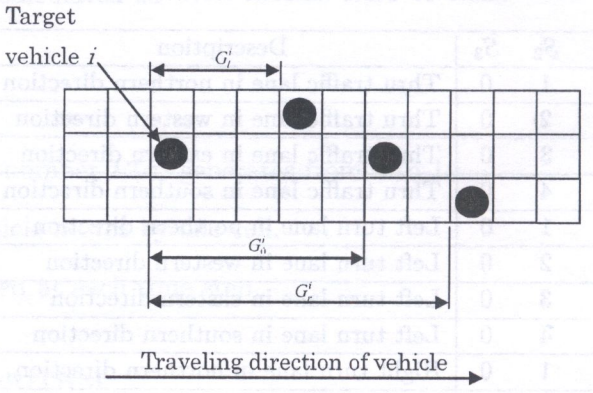

Fig. 2. Following vehicle distance

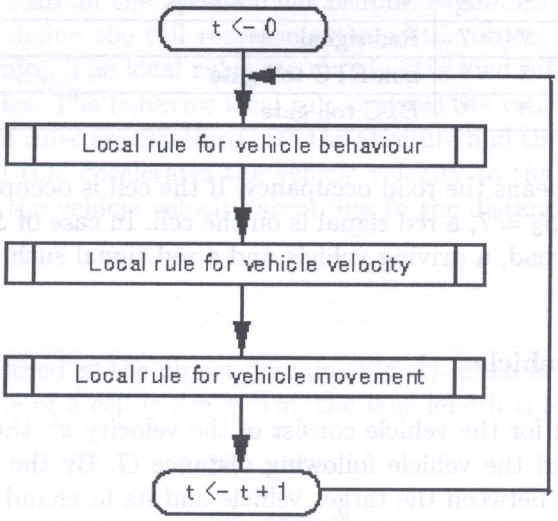

Fig. 3. Local rules

3.5.1. Behavior local rule

The behavior local rules consist of basic behavior local rules for going ahead, turning right, turning left, changing lanes and stopping. Since the object domain is two-lane road, the turning right and left are not used in the numerical examples.

Different behavior local rules are switched according to the distance between the target vehicle and the gate. If the distance between the target vehicle and the gate is greater than 370 m or after the vehicle passes over the gate, the behavior local rule 1 (Fig. 5) is applied. If not so, the behavior local rule 2 (Fig. 6) is applied to all vehicles. The threshold 370 m is specified according to [23].

By the way, the cells C_N, C_{NE}, C_{NW}, C_E, and C_W are defined as in Fig. 4 in order to define the local rule.

(1) Behavior local rule 1

If the distance between the target vehicle and the gate is greater than 370 m or after the vehicle passes over the gate, the vehicle behavior is controlled with the local rule shown in Fig. 5. In the figure, the function $\max(G_r^i, G_0^i, G_l^i)$ indicates the maximum number among them.

If $G_0^i < G_s^i$ and if $G_r^i < G_l^i, G_0^i$, the vehicle is controlled with the local rule for changing right lane. After changing the lane, the vehicle is controlled with the local rule for going ahead.

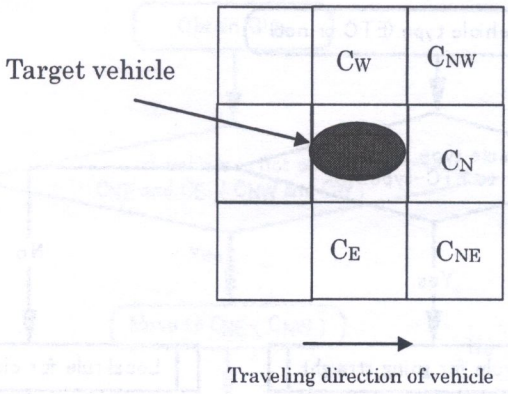

Fig. 4. Definition of cells which a vehicle moves to

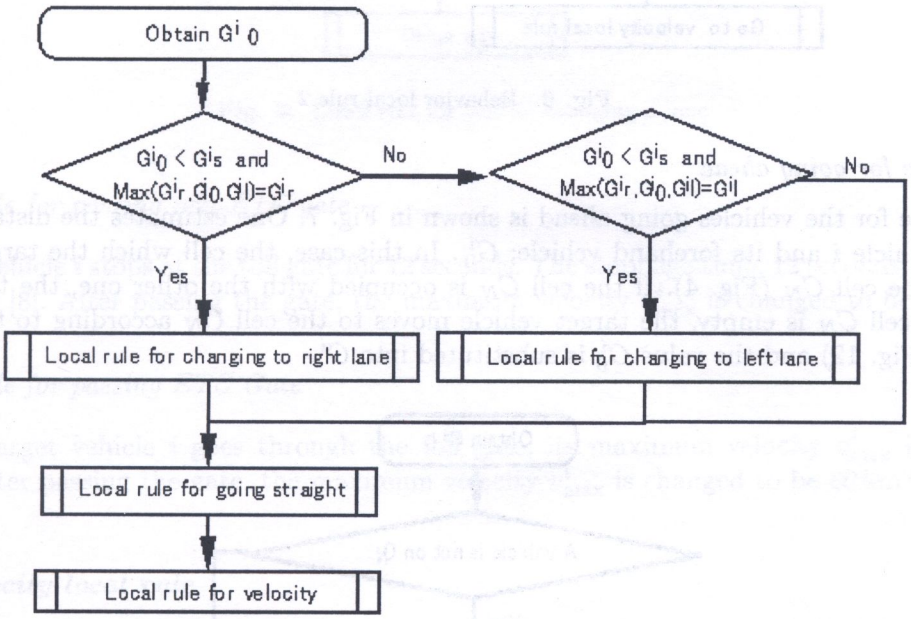

Fig. 5. Behavior local rule 1

If $G_0^i < G_s^i$ and if $G_l^i < G_r^i$, G_0^i, the vehicle is controlled with the local rule for changing left lane. After changing the lane, the vehicle is controlled with the local rule for going ahead.

If $G_0^i < G_s^i$ or if G_0^i is the greatest among them, the vehicle is controlled with the local rule for going ahead.

In the others, the vehicle stops.

(2) Behavior local rule 2

If the distance between the target vehicle and the gate is equal to or less than 370 m, the vehicle behavior is controlled with the local rule shown in Fig. 6.

If an ETC vehicle is going to an ETC gate or a non-ETC vehicle is going to a non-ETC gate, the vehicle is controlled with the local rule for going ahead.

If an ETC vehicle is going to a non-ETC gate or a non-ETC vehicle is going to an ETC gate, the vehicle is controlled with the local rule for changing lane. After changing the lane, it is controlled with the local rule for going ahead.

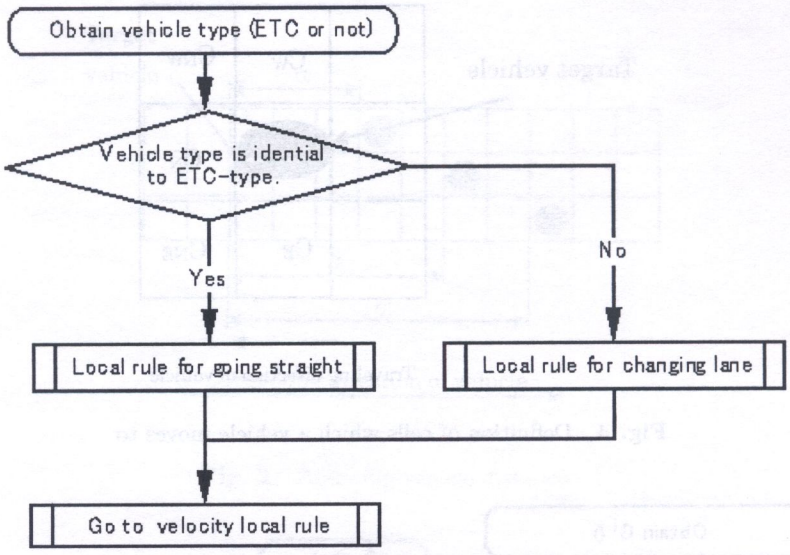

Fig. 6. Behavior local rule 2

(3) Local rule for going ahead

The local rule for the vehicles going ahead is shown in Fig. 7. One estimates the distance between the target vehicle i and its forehand vehicle; G_0^i. In this case, the cell which the target vehicle is going to is the cell C_N (Fig. 4). If the cell C_N is occupied with the other one, the target vehicle stops. If the cell C_N is empty, the target vehicle moves to the cell C_N according to the local rule for moving (Fig. 12) and the value G_0^i is substituted into G^i.

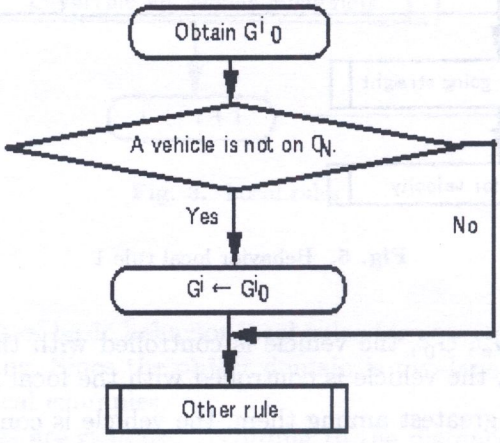

Fig. 7. Local rule for vehicle going ahead

(4) Local rule for changing driving lane

The local rule for changing a lane is shown in Fig. 8. The symbols without bracket are related to the local rule for changing to the right lane and the symbols with bracket are to the rule for changing to the left lane.

One estimates the distance between the target vehicle i and its forehand vehicle G_0^i. The cell which the target vehicle is going to is the cell C_{NE} or C_{NW} (Fig. 4). If the cell C_{NE} or C_{NW} is occupied with the other vehicle, the target vehicle is controlled with the other rules than the rule for changing lane. If the cell C_{NE} or C_{NW} is empty, the target vehicle changes the driving lane and the value G_r^i or G_l^i is substituted into G^i.

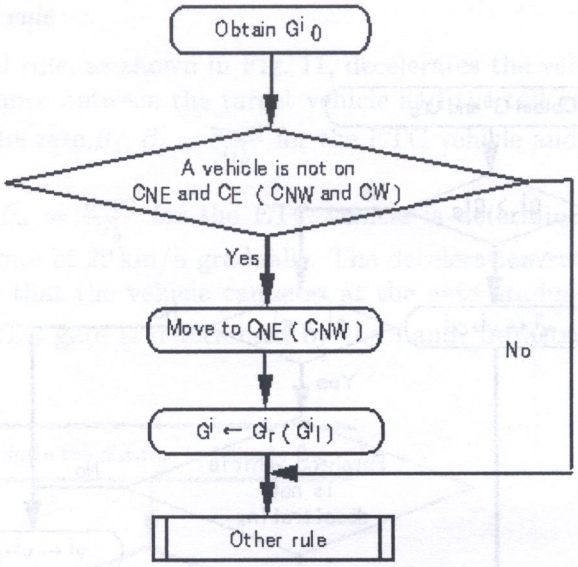

Fig. 8. Local rule for vehicle changing a lane

(5) Local rule for passing non-ETC gate

The target vehicle i stops at the toll gate for 12 seconds. The stoppage time, 12 seconds, is determined according to [8]. After passing the gate, the maximum velocity $v^i_{\max}$ is changed to be 80 km/h.

(6) Local rule for passing ETC Gate

When the target vehicle i goes through the toll gate, its maximum velocity $v^i_{\max}$ is specified as 20 km/h. After passing the gate, the maximum velocity $v^i_{\max}$ is changed to be 80 km/h.

3.5.2. Velocity local rule

The velocity local rule consists of the absolute and the relative velocity local rules. The absolute local rule performs for the target vehicle to decelerate safely to the toll gate and the relative local rule changes the vehicle velocity according to the vehicle following distance.

(1) Relative velocity local rule

The relative velocity local rule, as shown in Fig. 9, changes the vehicle velocity according to the magnitude relation between the following vehicle distance G^i and the safety following vehicle distance G^i_s calculated from the vehicle velocity v.

If $G^i > G^i_s$, the vehicle velocity is increased by the rate α.

If $G^i < G^i_s$, the vehicle velocity is decreased by the rate β.

If $G^i = G^i_s$ and if the forehand vehicle is decelerating, the vehicle velocity is decreased by the rate β.

If $v^i > v^i_{max}$, $v^i \leftarrow v^i_{max}$ and if $v^i < 0$, $v \leftarrow 0$.

Besides, the rate α and the rate β are determined from the actual estimated data [26]. Figure 10a shows the relationship between the acceleration rate $\alpha\,(\mathrm{m/s^2})$ and the velocity $v\,(\mathrm{km/h})$ when the vehicles accelerate actually. Figure 10b shows the relationship between the deceleration rate $\beta\,(\mathrm{m/s^2})$ and the following vehicle distance $G(m)$ when the vehicles decelerate actually.

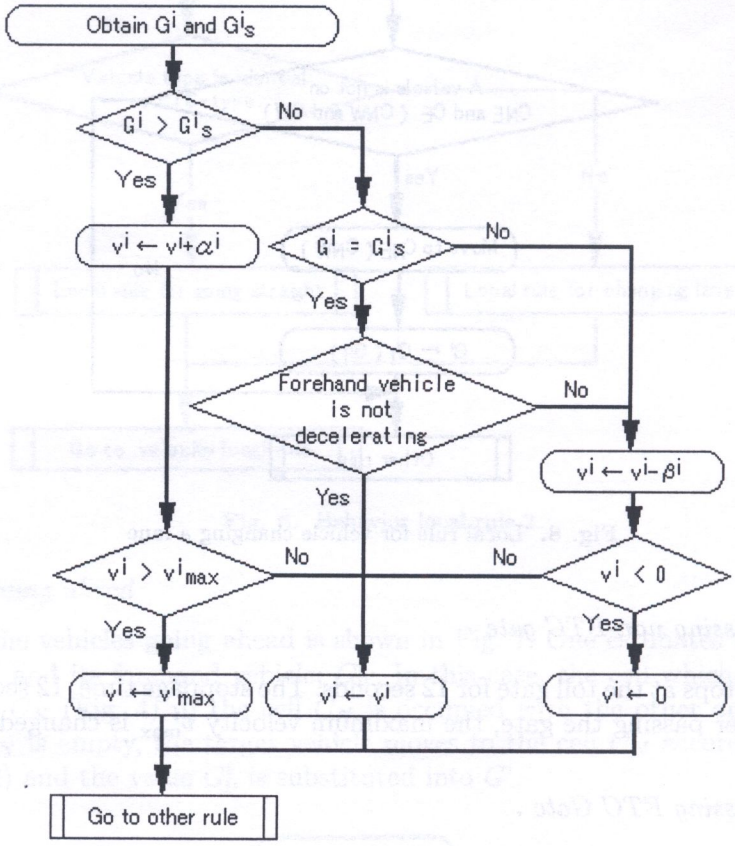

Fig. 9. Relative velocity local rule

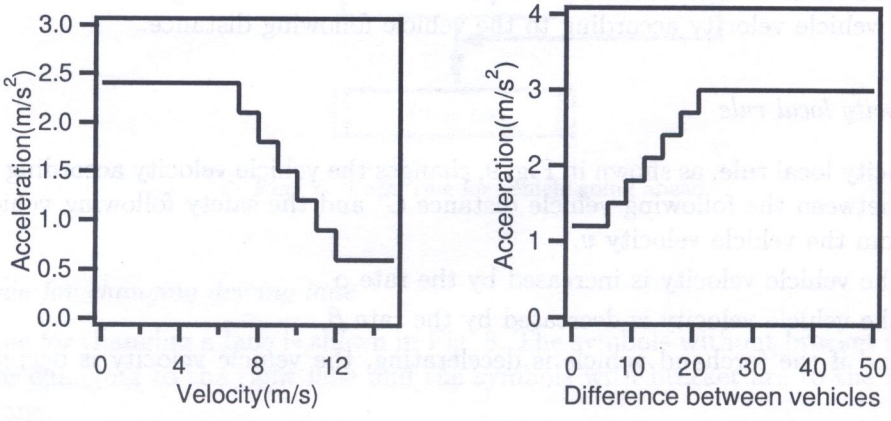

(a) Acceleration rate (b) Deceleration rate

Fig. 10. Acceleration and deceleration rate

(2) Absolute velocity local rule

The absolute velocity local rule, as shown in Fig. 11, decelerates the vehicle to the toll gate.

One estimates the distance between the target vehicle and the toll gate G_g^i. If $G_g^i < 370\,\mathrm{m}$, the vehicle is decelerated by the rate β_g; $\beta_g = \frac{v-20}{G_g^i}$ for the ETC vehicle and $\beta_g = \frac{v}{G_g^i}$ for the non-ETC vehicle, respectively.

The deceleration rate $\beta_g = \frac{v-20}{G_g^i}$ for the ETC vehicle is determined so that the vehicle can approach the gate at the rate of 20 km/h gradually. The deceleration rate for the non-ETC vehicle $\beta_g = \frac{v}{G_g^i}$ is determined so that the vehicle can stop at the gate gradually. The velocity when the ETC vehicle passes the ETC gate is determined by the Land, Infrastructure and Transportation Ministry of Japan.

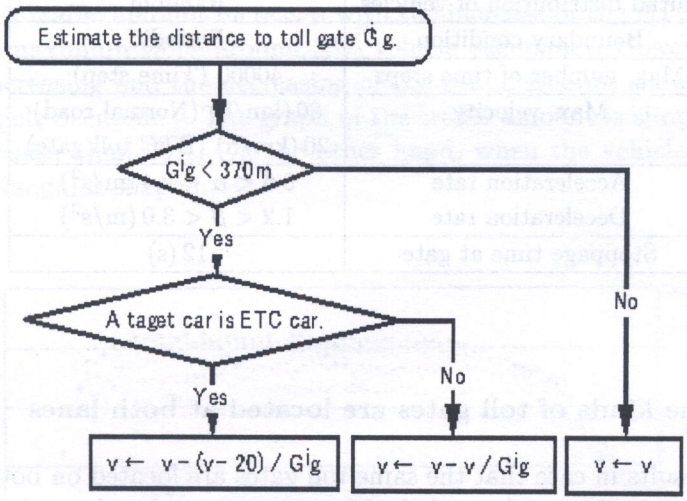

Fig. 11. Absolute velocity local rule

3.6. Local rule for movement

The local rule for movement moves the vehicles according to the concept of the stochastic velocity model described in the section 2.2.5. The algorithm of the local rule is shown in Fig. 12.

The moving probability of the vehicle P_0 is calculated from the velocity v. The uniform real random number $P(x)$ is generated from 0 to 1. If $P(x) < P_0$, the vehicle moves by one cell and contrariwise, the vehicle stops.

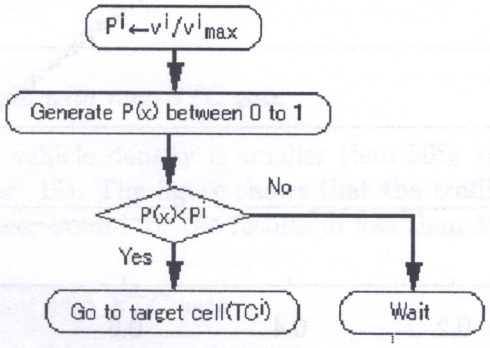

Fig. 12. Local rule for movement

4. Numerical example

The parameters for the simulation are shown in Table 2. The acceleration rate α and β are taken from the reference [26]. The vehicles are distributed randomly at the initial time step. The periodic boundary conditions are specified at both ends of the object domain. In the periodic condition, the vehicles passing through the right end come into the domain from the left end again. The periodic boundary condition can keep the vehicle density at the constant value.

Table 2. Simulation parameters

Cell size	3 (m)
1 time step	0.1 (s)
Initial distribution of vehicles	Random
Boundary condition	Periodic
Max. number of time steps	40000 (Time step)
Max. velocity	80 (km/h) (Normal road) 20 (km/h) (ETC toll gate)
Acceleration rate Deceleration rate	$0.6 < \alpha < 2.4\,(\mathrm{m/s^2})$ $1.2 < \beta < 3.0\,(\mathrm{m/s^2})$
Stoppage time at gate	12 (s)

4.1. In case that same kinds of toll gates are located at both lanes

We shall consider the results in case that the same toll gates are located on both lanes of a two-lane road (Fig. 13). The results in the two-lane road without gates are also shown in the same figure. The abscissa and the ordinate denote the vehicle occupancy (%) and the traffic amount (vehicles/hour), respectively. The vehicle occupancy is evaluated as the percentage of the road cells occupied with vehicles in all cells. The traffic amount is evaluated as the number of the driving vehicles per one hour. The traffic amount in case of the no toll gate increases till 20% vehicle occupancy and then,

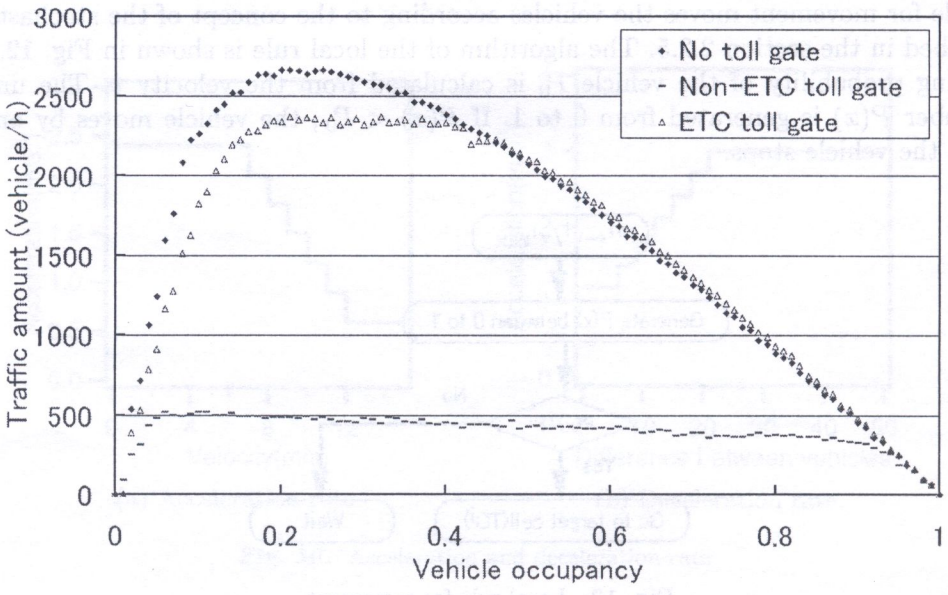

Fig. 13. In case that same kind of gates set at each lane

decreases gradually. The result of the ETC gate shows the similar tendency to that of the no toll gate but its maximum traffic amount is smaller than that of the no toll gate by 10%. In the result of the normal toll gate, the maximum traffic amount is about 20% of that of the no toll gate.

The results indicates that the maximum traffic amount depends on the capacity of the toll gate, and the ETC gate is very available for fixing the traffic congestion due to the toll gate.

4.2. In case that the different kind of toll gate is located at each lane

We shall consider the results in case that the non-ETC and ETC gate is located at individual lane, respectively (Fig. 14).

We notice that the traffic amount increases with the increase of the ETC vehicles and the traffic amount reaches the maximum value around 30% vehicle occupancy. However, the more important aspect is that the increasing and the decreasing of the traffic amount shows the different tendency according to the vehicle occupancy. The graph of the traffic amount is simply trapezoidal when the vehicle density is greater than 50%. On the other hand, when the vehicle density is smaller than 50%, the graph is triangular-shaped.

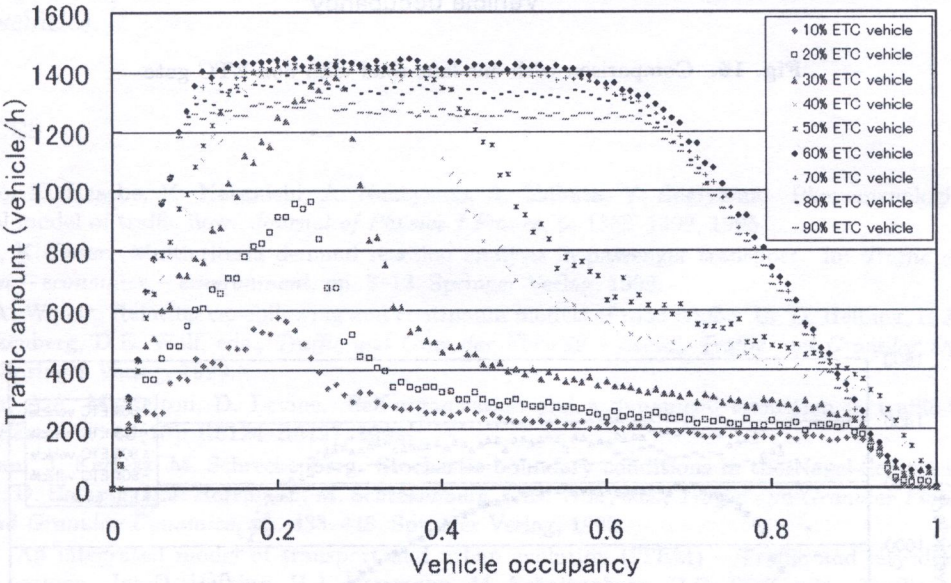

Fig. 14. In case that the different kind of gate is located at each lane.

Comparison with one-lane road with non-ETC gate

The results in case that the vehicle density is smaller than 50% are compared with the one-lane road with non-ETC gate (Fig. 15). The figure shows that the traffic amount in the one-lane road with non-ETC gate is the lower bound for the results in less than 50% vehicle density.

Comparison with one-lane road with ETC gate

The results in case that the vehicle density is greater than 50% are compared with the one-lane road with ETC gate (Fig. 16). The figure shows that the traffic amount in the one-lane road with ETC gate is the upper bound for the results in greater than 50% vehicle density.

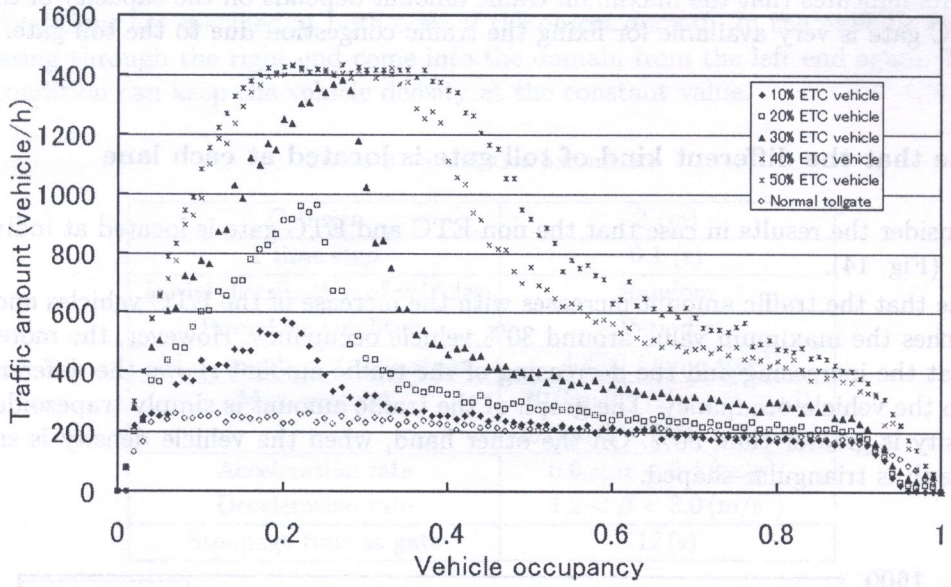

Fig. 15. Comparison with one-lane road with non-ETC gate

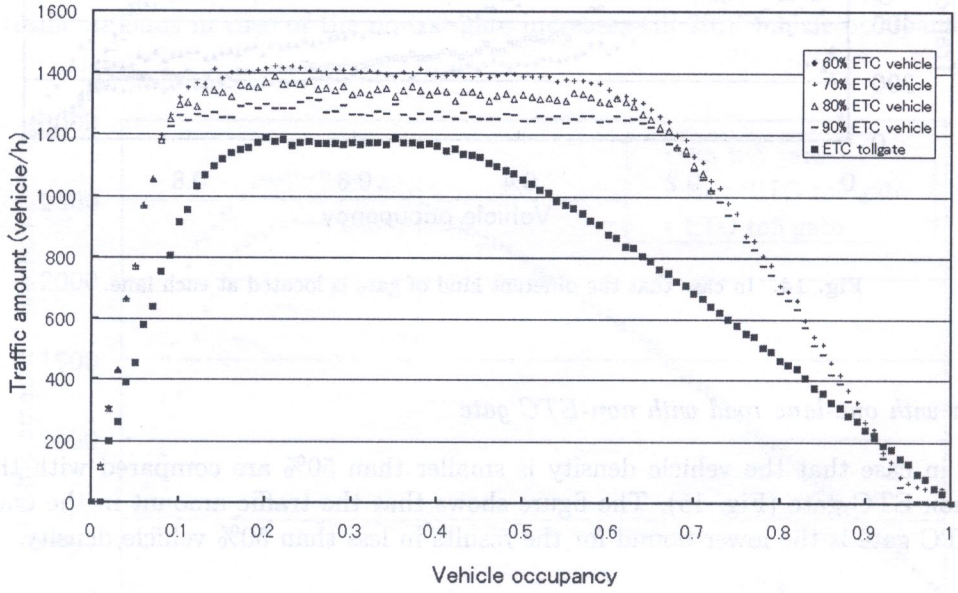

Fig. 16. Comparison with one-lane road with ETC gate

5. Conclusion

This paper describes the simulation of the traffic flow through the toll gate by using the cellular automata and the stochastic velocity model.

A two-lane road was considered as the numerical example and the ETC and the non-ETC gates were located at a lane to discuss the effect of the toll gate for the traffic amount.

First, we discussed the results in case that the same kind of gates are located at each lane. The maximum traffic amount in the ETC gate is smaller by about 10% than that in the no gate. In the non-ETC gate, the maximum traffic amount is smaller by at least 80% than that of the no gate. The results indicates that the maximum traffic amount depends on the capacity of the toll gate and therefore, the ETC gate has the great availability for fixing the traffic congestion due to the toll gate.

Next, we compared the results in case that the non-ETC and ETC gates are located at individual lane, respectively. The traffic amount depends on the rate of the ETC-vehicles among all driving vehicles. In the ETC-vehicle density of less than 50%, the traffic amount in the one-lane road with non-ETC gate is the lower bound. On the other hand, in the ETC-vehicle density of greater than 50%, the traffic amount in the one-lane road with ETC gate is the upper bound.

The traffic amount depends not only on the number of the driving vehicles but also the type of vehicles and therefore, we can conclude that the number and the type of the toll gates should be determined according to the the vehicle occupancy and the percentage of the ETC vehicles among the driving vehicles.

References

[1] M. Bando, K. Hasebe, K. Nakanishi, A. Nakayama, A. Shibata, Y. Sugiyama. Phenomenological study of dynamical model of traffic flow. *Journal of Physics I France*, **5**: 1389–1399, 1995.

[2] H. Baum, K. Esser. Multicriteria demand reaction analysis in passenger transport. In: *Traffic and Mobility: simulation – economics – environment*, pp. 3–12. Springer Verlag, 1999.

[3] P. Berg, A. Woods. Relating car-following and continuum models of road traffic. In: D. Helbing, H.J. Herrmann, M. Schrekenberg, D.E. Wolf, eds., *Traffic and Granular Flow'99 – Social, Traffic and Granular Dynamics*, pp. 389–394. Springer Verlag, 1999.

[4] O. Biham, A.A. Middelton, D. Levine. Self-organization and a dynamical transition in traffic-flow models. *Physical Review A*, **46**(10): R6124–R6127, 1992.

[5] S. Cheybani, J. Kertesz, M. Schreckenberg. Stochastic boundary conditions in the Nagel-Schreckenberg traffic model. In: D. Helbing, H.J. Herrmann, M. Schrekenberg, D.E. Wolf, eds., *Traffic and Granular Flow'99 – Social, Traffic and Granular Dynamics*, pp. 433–448. Springer Verlag, 1999.

[6] G. Haag. An integrated model of transport and urban evolution (ITEM) – Traffic and city development in emergent nations. In: D. Helbing, H.J. Herrmann, M. Schrekenberg, D.E. Wolf, eds., *Traffic and Granular Flow'99 – Social, Traffic and Granular Dynamics*, pp. 285–306. Springer Verlag, 1999.

[7] K. Hasebe, A. Nakayama, Y. Sugiyama. Exact traveling cluster solutions of differential equations with delay for a traffic flow model. In: D. Helbing, H.J. Herrmann, M. Schrekenberg, D.E. Wolf, eds., *Traffic and Granular Flow'99 – Social, Traffic and Granular Dynamics*, pp. 413–418. Springer Verlag, 1999.

[8] Infrastructure Road Bureau, Land and Transportation Ministry of Japan. http://www.mlit.go.jp/road/ITS/j-html/index.html

[9] Y. Ishibashi, M. Fukui. Temporal variations of traffic flow in the Biham-Middleton-Levine method. *Journal of the Physical Society of Japan*, **63**(8): 2882–2885, 1994.

[10] i Transport Lab. City traffic flow simulation model AVENUE. http://www.i-transportlab.jp/products/avenue/

[11] B.S. Kerner. Phase transitions in traffic flow. In: D. Helbing, H.J. Herrmann, M. Schrekenberg, D.E. Wolf, eds., *Traffic and Granular Flow'99 – Social, Traffic and Granular Dynamics*, pp. 253–284. Springer Verlag, 1999.

[12] A. Kittel, A. Eidmann, M. Goldbach. Detailed microscopic rules to simulate multilane freeway traffic. In: D. Helbing, H.J. Herrmann, M. Schrekenberg, D.E. Wolf, eds., *Traffic and Granular Flow'99 – Social, Traffic and Granular Dynamics*, pp. 425–430. Springer Verlag, 1999.

[13] W. Knospe, L. Santen, A. Schadschneider, M. Schreckenberg. CA models for traffic flow: Comparison with empirical single-vehicle data. In: D. Helbing, H.J. Herrmann, M. Schreckenberg, D.E. Wolf, eds., *Traffic and Granular Flow'99 – Social, Traffic and Granular Dynamics*, 431–436. Springer Verlag, 1999.

[14] H.Y. Lee, H.-W. Lee, D. Kim. Empirical phase diagram of traffic flow on highways with on-ramp. In: D. Helbing, H.J. Herrmann, M. Schrekenberg, D.E. Wolf, eds., *Traffic and Granular Flow'99 - Social, Traffic and Granular Dynamics*, pp. 345–350. Springer Verlag, 1999.

[15] M.J. Lighthill, G.B. Whitham. On kinematic waves II. A theory of traffic flow on long crowded roads. *Proceedings of Royal Society London*, **A299**: 317, 1955.

[16] T. Musha, H. Higuchi. Traffic current fluctuation and the Burgers equation. *Japan Journal of Applied Physics*, **17**: 811, 1978.

[17] K. Nagel, M. Schreckenberg. Cellular automaton model for freeway traffic. *Journal of Physics, I France*, **2**: 2221–2229, 1992.

[18] K. Nagel, S. Rasmussen. Traffic at the edge of chaos. In: R.A. Brooks, P. Maes, eds., *Artificial Life IV (Proc. 4th International Workshop on the Synthesis and Simulation of Living Systems)*, 222–235. The MIT Press, 1994.

[19] K. Nagel. Particle hopping models and traffic flow theory. *Physical Review E*, **53**(5): 4655–4672, 1996.

[20] National Transportation Library. TrafNetsim. http://ntl.bts.gov/DOCS/netsim.html

[21] L. Neubert, L. Santen, A. Schadschneiber, M. Schreckenberg. Statistical analysis of freeway traffic. In: D. Helbing, H.J. Herrmann, M. Schrekenberg, D.E. Wolf, eds., *Traffic and Granular Flow'99 - Social, Traffic and Granular Dynamics*, pp. 307–314. Springer Verlag, 1999.

[22] R. Sollacher, H. Lenz. Nonlinear control of stop-and-go traffic. In: D. Helbing, H.J. Herrmann, M. Schrekenberg, D.E. Wolf, eds., *Traffic and Granular Flow'99 - Social, Traffic and Granular Dynamics*, pp. 315–320. Springer Verlag, 1999.

[23] Special committee for driving technique for energy saving. Estimation of energy-saving effect of etc. http://www.eccj.or.jp/fuel/95/chapter_3/index.html

[24] Y. Sugiyama. Optimal velocity model for traffic flow. *Computer Physics Communications*, **121–122**, 399–401, 1999.

[25] T. Tamaki, S. Yasue, E. Kita. Traffic simulation using stochastic velocity model and CA (in Japanese). *Transaction of Information Processing Society in Japan*, **45**(3): 858–869, 2004.

[26] T. Tamaki, S. Yasue, E. Kita. City traffic simulation using cellular automata with stochastic velocity model. In: *Proceedings of The 2004 International Conference on Parallel and Distributed Processing Techniques and Applications (PDPTA2004)*, **12**: 440–441, 2004.

[27] I. Tanahashi, H. Kitaoka, M. Baba, H. Mori, S. Terada, E. Teramoto. Wide area traffic flow simulator NETSTREAM (in Japanese). In: *IPSJ, ITS*, **9**(2): 9–14, 2002.

[28] B. Tilch, D. Helbing. Evaluation of single vehicle data in dependence of the vehicle-type, lane and site. In: D. Helbing, H.J. Herrmann, M. Schrekenberg, D.E. Wolf, eds., *Traffic and Granular Flow'99 - Social, Traffic and Granular Dynamics*, pp. 333–338. Springer Verlag, 1999.

[29] E. Tomer, L. Safonov, S. Havlin. Stable and metastable states in congested traffic. In: D. Helbing, H.J. Herrmann, M. Schrekenberg, D.E. Wolf, eds., *Traffic and Granular Flow'99 - Social, Traffic and Granular Dynamics*, pp. 419–424. Springer Verlag, 1999.

[30] Toyota Central Laboratory. NETSTREAM. http://www.tytlabs.co.jp/office/library/lib_01/netstream/

[31] M. Treiber, A. Hennecke, D. Helbing. Microscopic simulation of congested traffic. In: D. Helbing, H.J. Herrmann, M. Schrekenberg, D.E. Wolf, eds., *Traffic and Granular Flow'99 - Social, Traffic and Granular Dynamics*, pp. 365–376. Springer Verlag, 1999.

[32] S. Wolfram. *Cellular Automata and Complexity*. Addison-Wesley Publishing Company, 1 ed., 1994.

[33] S. Yukawa, M. Kikuchi. Coupled-map modeling of one-dimensional traffic flow. *Journal of the Physical Society of Japan*, **64**(1): 35–38, 1995.